SUPPLEMENTARY MATERIALS

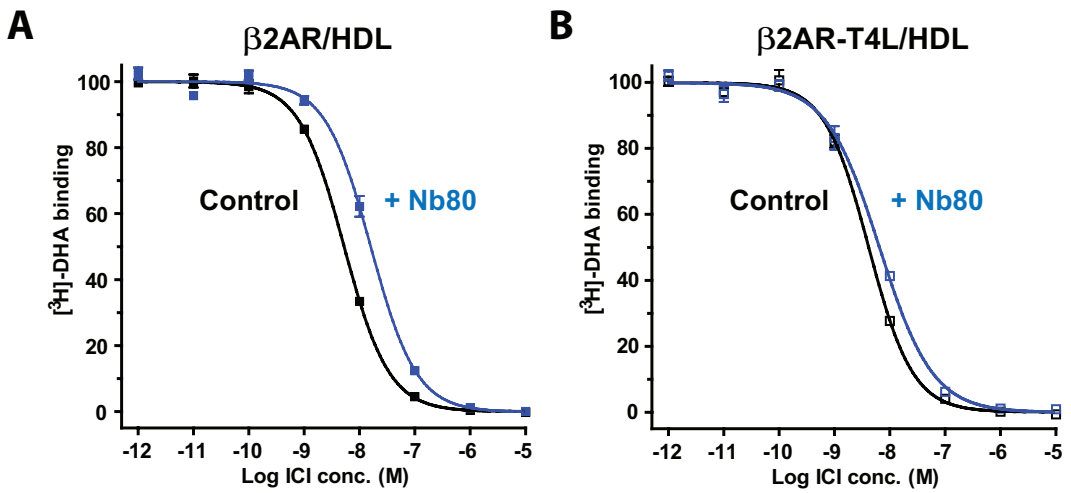

Supplementary Figure 1. Ligand binding curves for the inverse agonist ICI-118551 competing against [^{3}H]-dihydroalprenolol ([^{3}H]-DHA) for **a**, β_2AR/HDL in the absence and presence of Nb80, and **b**, β_2AR-T4L/HDL in the absence and presence of Nb80.

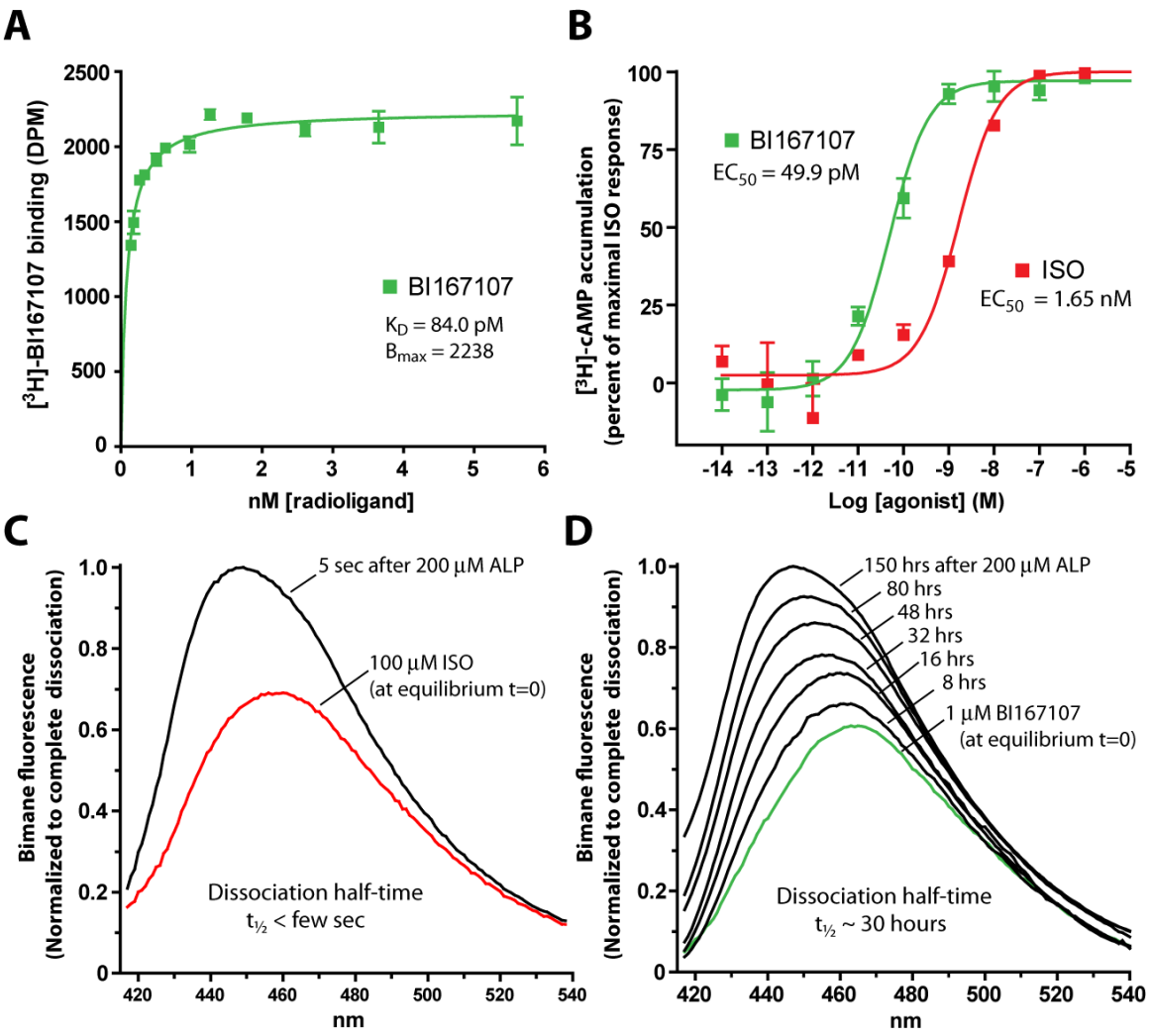

Supplementary Figure 2. Pharmacological characterization of the BI-167107 agonist **a**, Saturation binding curve for [^{3}H]-BI-167107. **b**, The efficacy of BI-167107 was determined by [^{3}H]-cAMP accumulation in CHO cells expressing human β_2AR. BI-167107 elicits the same full stimulatory response as (-)-isoproterenol (ISO), but with a higher potency. **c**, Fluorescence emission spectra showing complete dissociation of ISO from bimane labeled β_2AR within 5 seconds of adding a competitive amount of the antagonist alprenolol (ALP). **d,** BI-167107 dissociates with a half-time of about 30 hours from the bimane labeled β_2AR and reaches completion 150 hours after addition of ALP.

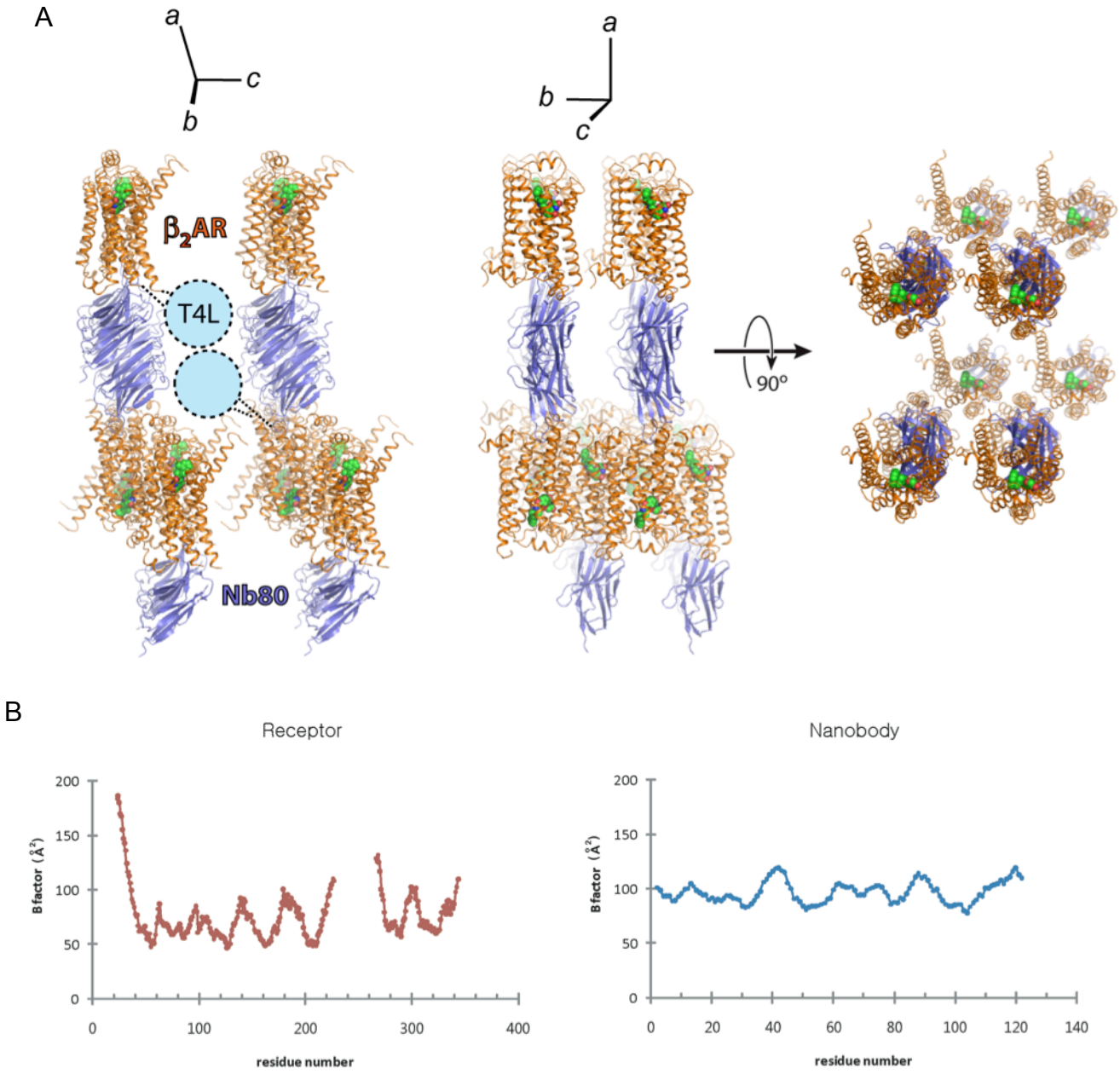

Supplementary Figure 3. Packing of the agonist-β_2AR-T4L-Nb80 complex in crystals formed in lipidic cubic phase. **a,** Three different views of the structure of β_2AR indicated in orange, Nb80 in blue, and BI-167107 agonist in green. The β_2AR-nanobody complexes are arranged with the lipid bilayers approximately parallel to the *bc* plane of the crystal. Twofold symmetry related nanobody molecules interact along the *a* axis to generate a tightly packed lattice in this

direction. Within the bilayer, receptor molecules interact in an antiparallel arrangement with TM1,2,3 and 4 of one β_2AR molecule packing against TM4 and 5 of the adjacent molecule. Contacts are also made between helix 8 and TM5 of parallel lattice neighbor along the *b* axis, and between the extracellular portion of TM1 and the cytoplasmic end of TM6 of a third, antiparallel neighbor. The packing is weakest along the *c* axis, which may be due in part to non-specific interactions of the T4L with neighboring receptor and/or nanobody molecules. There is no interpretable electron density for the T4L, but given the visible ends of TM5 and TM6 the position of T4L is highly constrained. Its likely position is indicated by the light blue circle with black dashed lines connected to the intracellular ends of TM5 and TM6 where it is fused in the β_2AR-T4L construct. Presumably T4L adopts a number of orientations relative to the receptor, and perhaps a range of internal conformations due to its hinge motion[1], that average out its density. Nonetheless, T4L likely contributes to the structure of the crystal since we were unable to produce crystals of the native β_2AR-nanobody complex under these conditions, although it is possible that the flexible loop that connects TM5 and TM6 in the native receptor prevents lattice formation. PyMOL (http://www.pymol.org) was used for the preparation of all structure figures.

b, Plot of average temperature factor versus residue number. The β_2AR and nanobody are shown separately. The average temperature factors for receptor residues are lower than those of the nanobody, consistent with the more extensive interactions of the receptor in the lattice. The average was taken over all atoms modeled in the residue, including main chain and side chain. Similar plots using only the main chain atoms are very similar (not shown).

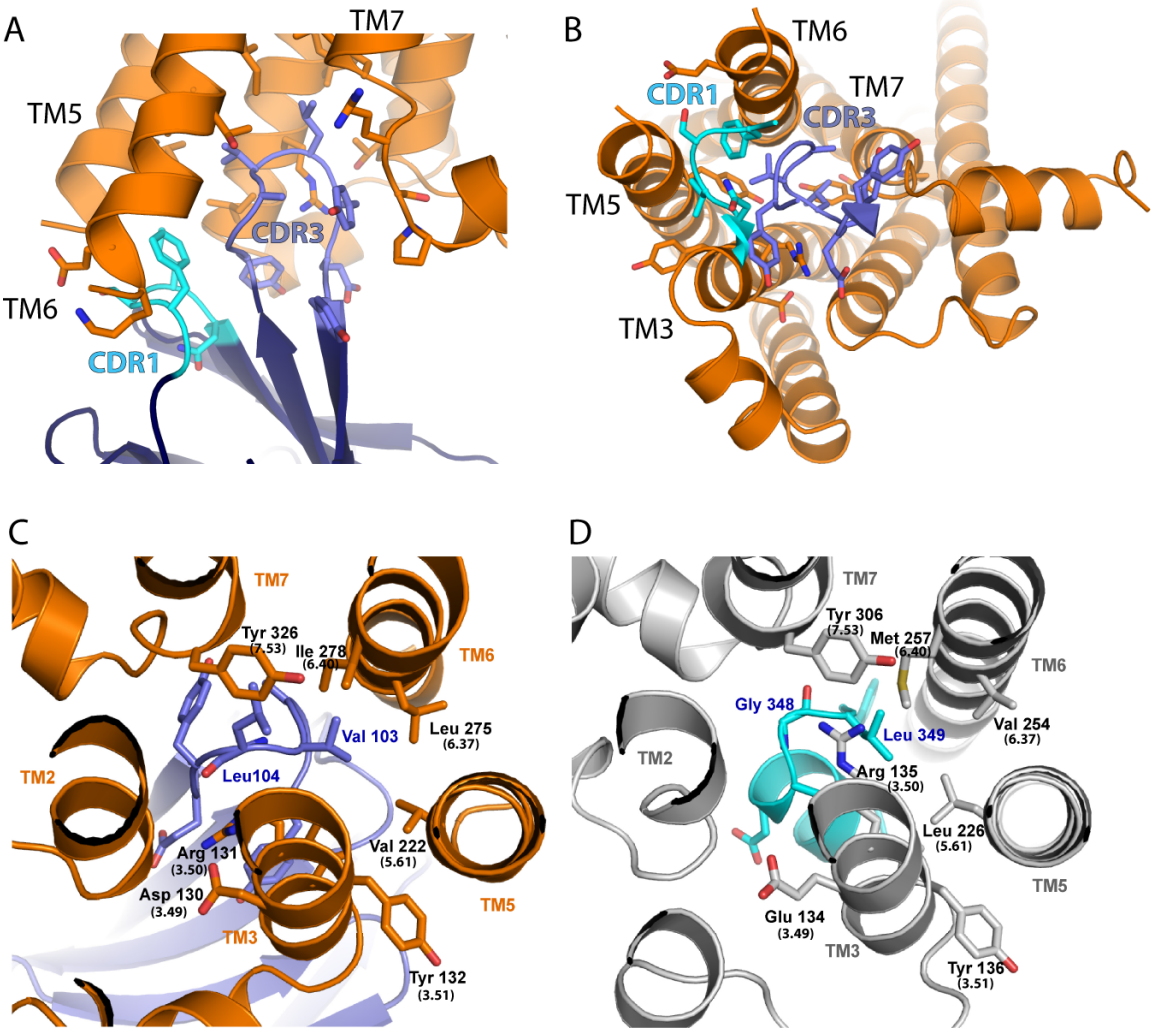

Supplementary Figure 4. Nb80 stabilized intracellular domain compared to and opsin structures. a, Side view of β_2AR (orange) with CDRs of Nb80 in light blue (CDR1) and blue (CDR3) that have amino acids within 4Å of the receptor. Side chains in TM3, 5, 6, and 7 within 4 Å of the CDRs are shown. The longer CDR3 loop penetrates 13 Å into the receptor. **b**, Interaction of CDR1 and CDR3 viewed from the intracellular side. **c**. Interactions between the β_2AR and Nb80 viewed from within the transmembrane domains of the β_2AR. **d**. Interactions between opsin and the carboxyl terminal peptide of transducin.

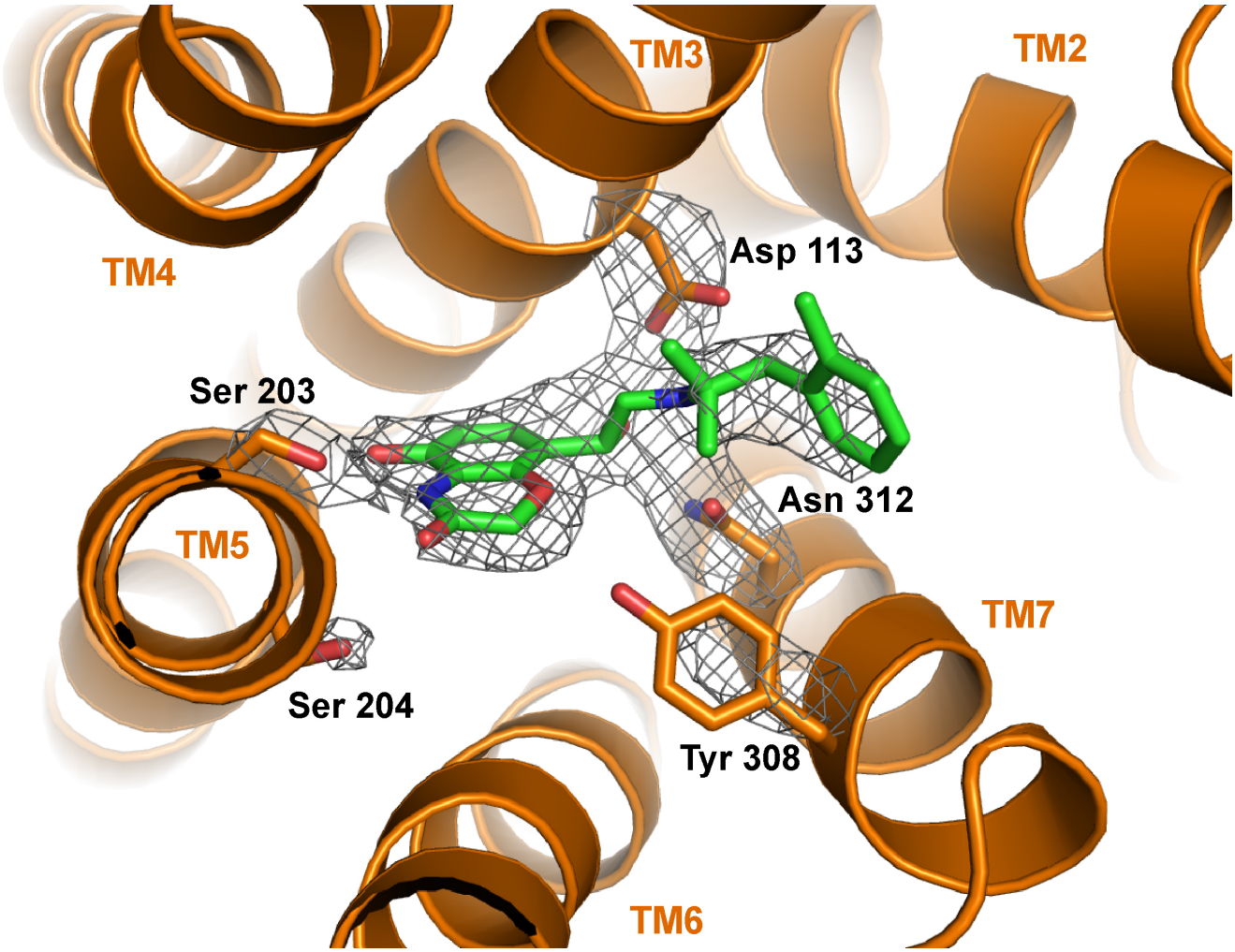

Supplementary Figure 5. Electron density map of agonist binding pocket. An omit map was calculated by removing the ligand and the labeled side chains from the model, then subjecting the model to a 2000 K simulated annealing run followed by minimization. The resulting F_{obs}-F_{calc} map is contoured at 2.5σ.

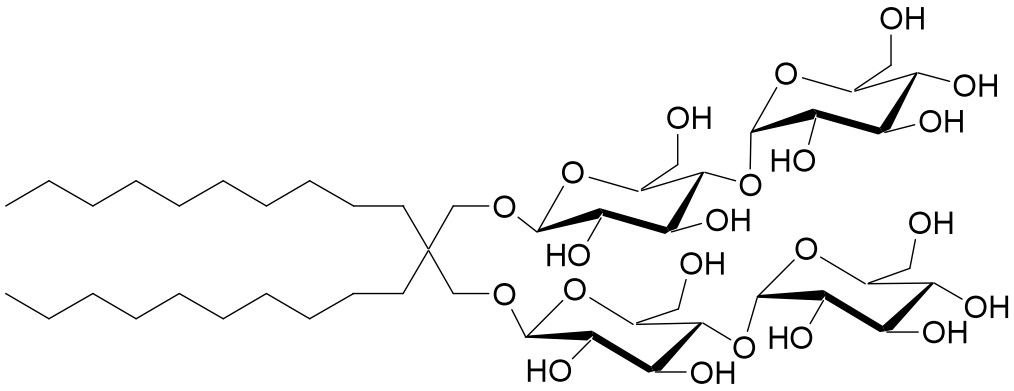

Supplementary Figure 6. Chemical structure of MNG3. The detergent MNG3 (11,11-Bis-β-D-maltopyranosidylmethyl-heneicosane) was used to stabilize purified β_2AR.

Supplementary Table S1. Pharmacological characterization of β_2AR reconstituted in HDL particles in complex with Gs and Nb80

	[^{3}H]-DHA saturation binding	[^{3}H]-DHA / ICI118,551 competition binding	[^{3}H]-DHA / (-)-isoproterenol competition binding		
	K_d ± S.E.		Low affinity state K_i [S.E. interval]	High affinity state K_i [S.E. interval]	
	nM	nM	nM	nM	
β_2AR	0.55 ± 0.09 (n=3)	2.52 [2.46 - 2.59] (n=3)	107.5 [103.8 - 111.3]		(n=3)
β_2AR + Gs			95.3 [82.8 – 109.7]	1.07 [0.96-1.19][1]	(n=4)
β_2AR + Gs + GTPγS			95.2 [92.2 - 98.3]		(n=3)
β_2AR + Nb80		7.6 [7.3 – 8.0] (n=3)		1.13 [1.09 - 1.18]	(n=3)
β_2AR-T4L	0.42 ± 0.01 (n=3)	1.71 [1.65 - 1.78] (n=3)	33.5 [31.6-35.5]		(n=3)
β_2AR-T4L + Nb80		2.69 [2.55 - 2.83] (n=3)		0.56 [0.54 - 0.57]	(n=4)

[1] 55 % of β_2AR population in high affinity state.

Supplementary Table S2 X-ray data collection and refinement statistics

A. Data collection statistics

wavelength (Å)	1.0332
space group	C2
unit cell parameters	
a (Å)	236.7
b (Å)	45.7
c (Å)	71.4
β (°)	102.3
number of crystals	23
resolution (Å)	37-3.50 (3.56-3.50)
unique reflections	10147 (903)
completeness (%)	94.8 (93.7)
multiplicity	3.5 (3.2)
$\langle I/\sigma(I)\rangle$	6.7 (1.8)
R_{merge}	0.192 (0.594)

B. refinement statistics

resolution (Å)	37-3.50
No. of reflections working set (test set)	9210 (937)
R_{work}/ R_{free}	0.225 / 0.294
rmsd from ideality	
bond lengths (Å)	0.010
bond angles (°)	1.3
Anisotropic B correction (Å^2)	B_{11}=33.5/B_{22}=2.7/B_{33}=-36.3/B_{13}=4.5
Average B factor (Å^2)	
receptor 76.4	
nanobody 96.6	
agonist 62.4	
Ramachandran analysis	
residues in most-favored region (%)	86.6
additionally allowed region (%)	13.4
generously allowed region (%)	0.0
disallowed region (%)	0.0

REFERENCES

1 Zhang, X. J., Wozniak, J. A. & Matthews, B. W. Protein flexibility and adaptability seen in 25 crystal forms of T4 lysozyme. *J Mol Biol* 250, 527-552 (1995).